Protoplasma (2010) 239:49–56
DOI 10.1007/s00709-009-0081-4

ORIGINAL ARTICLE

H_2O_2 localization in the green alga *Micrasterias* after salt and osmotic stress by TEM-coupled electron energy loss spectroscopy

Anza Darehshouri · Ursula Lütz-Meindl

Received: 21 August 2009 / Accepted: 19 October 2009 / Published online: 10 November 2009

Abstract Reactive oxygen species (ROS), including hydrogen peroxide (H_2O_2), are constantly generated as by-products of normal metabolic cellular pathways and can be over-produced in response to stress. In this study, we investigated ROS production and localization of H_2O_2 after salt (200 mM KCl) and osmotic (iso-osmotic sorbitol concentration) stress in the unicellular green alga *Micrasterias*. By means of the dye H_2DCFDA and confocal laser scanning microscopy, most ROS production could be detected in KCl-treated cells when compared to sorbitol-exposed cells and controls. For ultrastructural detection of H_2O_2, $CeCl_3$, which reacts with H_2O_2 and produces cerium perhydroxide deposits, has been used. Cerium was identified by transmission electron microscopy (TEM)-coupled electron energy loss spectroscopy (EELS) in organelles of KCl- and sorbitol-treated cells and in controls. Statistical measurements of the presence of the cerium $M_{4,5}$ edge were performed in mitochondria, chloroplasts, cell walls, and cytoplasmic sites of five individual cells after each treatment. The most pronounced increase in H_2O_2 production was found in chloroplasts of KCl- and sorbitol-treated cells. This shows that the chloroplast reveals the strongest response in H_2O_2 production after stress induction in *Micrasterias*. Significant elevation of H_2O_2 production also occurred in mitochondria and cytoplasm, whereas H_2O_2 levels remained unchanged or even slightly decreased in cell walls of treated cells. Additionally, TEM micrographs and EELS analyses provided indirect evidence for an increased H_2O_2 production at the plasma membrane of KCl-treated cells, indicating an involvement of the plasma membrane NADPH oxidase in H_2O_2 generation.

Keywords EELS · Cerium chloride · H_2O_2 · *Micrasterias* · TEM · KCl

A. Darehshouri · U. Lütz-Meindl (✉)
Plant Physiology Division, Cell Biology Department,
University of Salzburg,
Hellbrunnerstrasse 34,
5020 Salzburg, Austria
e-mail: ursula.luetz-meindl@sbg.ac.at

Present address:
A. Darehshouri
Department of Ecology and Evolutionary Biology,
University of Colorado,
Boulder, CO 80309, USA

Introduction

In aerobic organisms, reactive oxygen species (ROS) are part of the normal cellular metabolism (Pinto et al. 2003) and are produced in higher amounts as by-products of some metabolic pathways such as electron flows in mitochondria and chloroplasts (de Pinto et al. 2006; Tipathi et al. 2009). However, under unfavorable conditions, an early reaction is an enhanced production of ROS such as H_2O_2 (Doke et al. 1996). ROS have a dual function in plant cells. At higher concentrations, they damage the cells; but at moderate levels, they help the cells to adapt to various forms of stress by induction of an antioxidant response (Apel and Hirt 2004; Mazel et al. 2004; de Pinto et al. 2006; Boka et al. 2007; Chen et al. 2009). Although ROS are key players in signal pathways of cell death in animals, their precise role in plant cell death is still not clear. Numerous studies show that experimental exposure of plant cells to different concentrations of H_2O_2 may induce different cell death pathways from apoptotic-like cell death to necrosis (e.g., Houot et al. 2001; Gechev and Hille 2005; Gechev et al. 2006; de Pinto et al. 2006). For example, Houot et al. (2001) observed various features of programmed cell death (PCD) in tobacco BY-2 cells depending on the amount of H_2O_2 added to the

cultures. On the other hand, permanent ROS production at low levels does not induce cell death in tobacco cells (de Pinto et al. 2006) and may even increase cellular resistance in yeast (Costa and Moradas-Ferreira 2001).

The green alga *Micrasterias*, which has been used as cell biological model organism in numerous investigations, undergoes PCD upon treatment with H_2O_2 (Darehshouri et al. 2008). This is expressed in ultrastructural hallmarks such as slight chromatin condensation, deformation and disintegration of mitochondria, dilatation of cisternal rims of dictyosomes, as well as an increase in multivesicular bodies and in the number of endoplasmic reticulum (ER) compartments. Additionally, the activity of caspase-3 like enzymes is elevated, whereas photosynthetic activity drops down slightly.

Salt stress by increased osmolarity of the nutrient solution also causes marked ultrastructural alterations in *Micrasterias* and, at higher concentrations, inhibits or totally arrests cell division (Meindl et al. 1989). Induction of salt stress in *Micrasterias* by KCl leads to pronounced changes in organelle morphology and to formation of autophagosomes after long-term exposure (Affenzeller et al. 2009a, b). Both salt (KCl and NaCl) and osmotic (iso-osmotic sorbitol concentration) stress increase ROS production in *Micrasterias* cells and long-term salt stress evokes autophagic PCD (Affenzeller et al. 2009a, b).

The different biological responses which may be induced by ROS depend on several factors including the type of ROS, timing and intensity of the signal, and production sites (Gechev and Hille 2005; Paradiso et al. 2005; Gechev et al. 2006). This makes it particularly interesting to study subcellular localization of H_2O_2 at an ultrastructural level and to compare frequencies of H_2O_2 production at different organelles during stress response.

A successful, well-known technique for localization of H_2O_2 is a cytochemical method using cerium chloride ($CeCl_3$). $CeCl_3$ penetrates biological membranes both in plant and animal cells, reacts with H_2O_2, and produces insoluble cerium perhydroxide electron-dense deposits which can be visualized by conventional transmission electron microscopy (TEM; e.g., Bestwick et al. 1997; Pellinen et al. 1999; Waetzig et al. 1999; Blokhina et al. 2001; Köhler et al. 2001; Shinogi et al. 2002; Olmos et al. 2003; Musetti et al. 2005; Melillo et al. 2006; Boka et al. 2007; Zhang et al. 2008; Wu et al. 2009). Despite the fact that several studies have used the presence of precipitates as indicator for H_2O_2 production, only two investigations have so far unambiguously verified the presence of cerium by TEM-coupled electron energy loss spectroscopy (EELS; Köhler et al. 2001; Boka et al. 2007). Energy-filtering TEM represents a powerful tool for subcellular localization of elements and determination of bond states (Lütz-Meindl 2007) and has already been successfully employed in *Micrasterias* (Eder and Lütz-Meindl 2008) and other algae (Lütz-Meindl and Lütz 2006; Eder and Lütz-Meindl 2009).

In the present study, we investigate putative differences in ROS and H_2O_2 production after salt and osmotic stress. H_2O_2 localization is compared between different cell compartments and cytoplasmic sites in the green alga *Micrasterias* by statistical measurements of the cerium $M_{4,5}$ edge via EELS and by identification of cerium peroxide precipitates at an ultrastructural level.

Material and methods

Materials

All chemicals were purchased from Sigma-Aldrich (Vienna, Austria) or Roth (Karlsruhe, Germany), unless stated differently.

Cultivation and treatment

M. denticulata cells were grown in liquid Desmidiaceaen nutrient solution in Erlenmeyer flasks (Schlösser 1982) and kept at a constant temperature of 20°C and a 14:10-h light–dark regime. The cultures were subcultured every 4 to 5 weeks. Under these conditions, *Micrasterias* cells divide every 3 to 4 days by mitosis (for details, see Meindl et al. 1989). Cells of a defined stage (48 h after mitosis) were treated with 200 mM KCl or 339 mM sorbitol (iso-osmotic to KCl, measured) for 15 min (for details, see Affenzeller et al. 2009a).

ROS production

Control and treated cells were stained with 100 mM 2′,7′-dichlorofluorescein diacetate (H_2DCFDA; Invitrogen, Eugene, USA) for 45 min at room temperature. Cells were observed in a Zeiss Axiovert 100M equipped with a confocal laser scanner (LSM 510, Zeiss, Oberkochen, Germany). Samples were excited at 488 nm with an argon laser and viewed using a 505- to 550-nm band-pass filter. Zeiss LSM 510 software was used for image analysis. Each experiment was done with 50 cells and repeated three times.

Measurement of H_2O_2 production by $CeCl_3$ localization via EELS

For localization of H_2O_2, based on the generation of cerium perhydroxide, controls and treated cells were incubated in freshly prepared 5 mM $CeCl_3$ (Alfa Aesar, Emmerich, Germany) in 50 mM 3-(*N*-morpholino)-propane sulfonic acid (Mops) at pH 7.2 for 30 min at room temperature (Bestwick et al. 1997). Cells were fixed by high-pressure freeze fixation and subsequent cryosubstitution as described

previously (Meindl et al. 1992; Aichinger and Lütz-Meindl 2005) and were embedded in Agar low viscosity resin (LV Resin, VH1 and VH2 Hardener, and LV Accelerator; Agar Scientific, Essex, Great Britain). Fixation was done at least twice with different samples. Ultrathin sections (approx. 50 nm) were mounted on uncoated hexagonal narrow mesh copper grids for TEM analysis. Electron micrographs were captured in a LEO 912 TEM (Zeiss, Oberkochen, Germany), operated with a LaB_6 cathode and equipped with an in-column energy filter. Acceleration voltage of 80 kV was used for conventional imaging and 120 kV for EELS studies. For EELS measurements, illumination angles of 1 mrad, magnifications of 25.000 and exposure times of 5 s were used. Seven integration cycles were acquired for one measurement. The measuring area for EELS was defined by using a 100-µm spectrometer entrance aperture. The characteristic electron energy loss for the element cerium is 883 eV for the M_5 shell and 905 eV for the M_4 shell, resulting in a double peak. Mitochondria, chloroplasts, cell wall, and cytoplasmic sites of five individual cells were measured for each treatment. For statistical analysis, cerium was measured in ten samples of each organelle in each cell. H_2O_2 presence was also measured in some peroxisomes. TEM micrographs and EELS analysis were acquired by using a slow-scan dual-speed CCD camera TRS Sharpeye (Troendle, Moorenwies, Germany) controlled by the ITEM Software (Olympus-SIS, Soft Image System, Münster, Germany).

Statistics

The SigmaPlot software was used for statistical analyses and evaluation of standard errors (SE). The significance of measurements was determined by paired Student's *t* test. *P* value <0.05 was considered to be statistically significant.

Results

Production of ROS

To determine how many cells reveal ROS production after 15 min treatment with KCl or sorbitol, samples from control and treated cells were suspended in a cell permeable nonfluorescent H_2DCFDA dye. Intracellular esterases remove the acetate groups of this dye and subsequent oxidation changes it into a green fluorescent compound, which can be observed by confocal laser scanning microscopy. After 15 min treatment, a statistically significant increase of ROS production could be detected in 200 mM KCl-treated cells (about 66% of the cells) in comparison to controls (0%; Fig. 1). Increase in ROS production in the cells exposed to iso-osmotic sorbitol concentration was not significant (56% of the cells; Fig. 1).

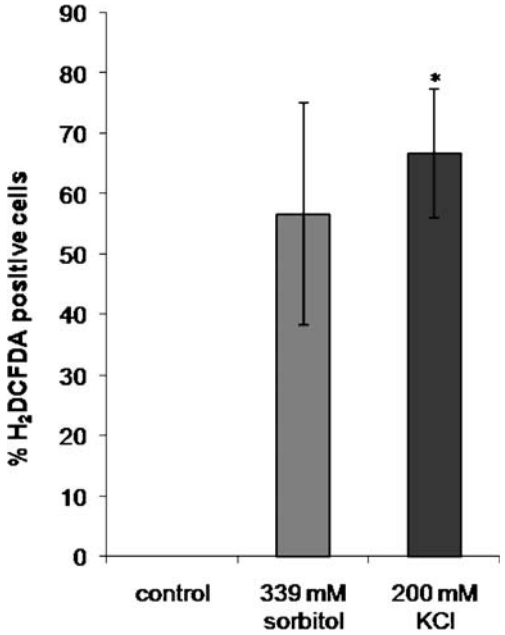

Fig. 1 ROS production measured by H_2DCFDA fluorescence in control *Micrasterias* cells and after 15 min treatment with 339 mM sorbitol (iso-osmotic to KCl) and 200 mM KCl in confocal laser scanning microscopy. Data are means of three independent experiments + SE. **P*<0.05

Subcellular localization of H_2O_2

Cerium chloride was used successfully in *Micrasterias* cells to detect H_2O_2 accumulation after stress induction. Precipitates of cerium perhydroxide at the plasma membrane of KCl-treated cells along the cell wall were clearly visible, but could not be observed in controls (Fig. 2a, b) or sorbitol-treated cells (data not shown). EELS measurements proved that the precipitates contained cerium. EEL spectra of this region have the characteristic double peak of the cerium $M_{4,5}$ edge (Fig. 2d), whereas control measurements at the cell wall did not reveal any cerium signal (Fig. 2c).

Statistical EELS analyses were carried out in mitochondria, chloroplasts, cell walls, and at different cytoplasmic sites of controls and treated cells (Fig. 3b, d, e, g, h). Cerium was identified at all measurement areas. However, the frequency of cerium presence was generally highest in KCl-treated cells, followed by sorbitol exposed cells and controls (Fig. 4). Chloroplasts of KCl-treated cells revealed a statistically significant increase in the frequency of cerium presence with an averaged factor of 2.1 when compared to controls. Additionally, the frequency of cerium measurements was also elevated in the cytoplasm (averaged factor 1.7) and in mitochondria (averaged factor 1.6) after KCl exposure. In sorbitol-treated cells, the increase in cerium measurements was also highest in chloroplasts (averaged factor 1.8) but only

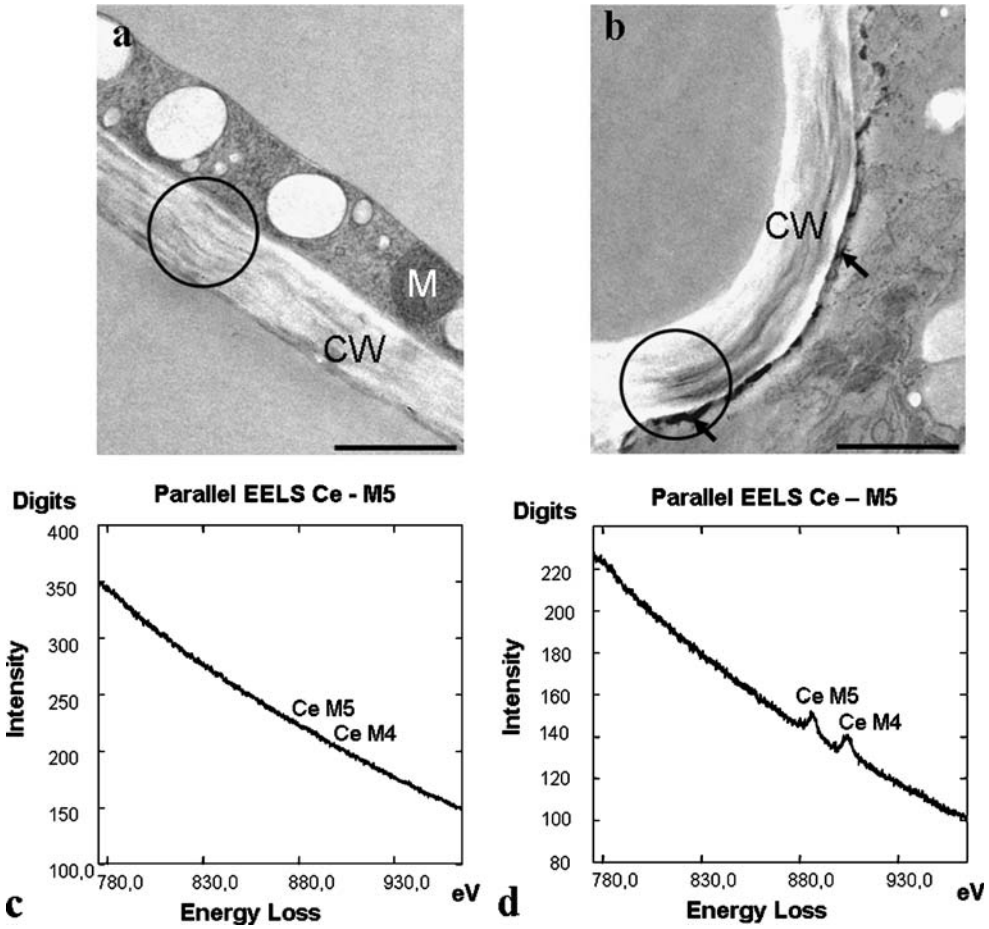

Fig. 2 TEM micrographs showing ultrastructure of *Micrasterias* cells pretreated with $CeCl_3$ for H_2O_2 localization: **a** control, **b** KCl-treated cell, cerium perhydroxide deposits at the plasma membrane (*arrows*). EEL spectra of the Ce $M_{4,5}$ edge from the *circled region* in **a** and **b**: **c** control cell, **d** KCl-treated cell. *CW* cell wall, *M* mitochondrion. Bar=1 μm

slight in mitochondria (averaged factor 1.3). In cell walls of KCl-treated cells, the frequency of cerium measurements was about the same as in controls but decreased with an averaged factor of 0.6 after sorbitol treatment. In summary, these results indicate that KCl induces the highest augmentation in H_2O_2 production in chloroplasts followed by the cytoplasm and by mitochondria. In chloroplasts of sorbitol-exposed cells, the increase in H_2O_2 production was also high. Mitochondria revealed only slightly elevated values and the amount of H_2O_2 production in the cytoplasm after sorbitol treatment was about the same as in controls. As expected, EELS studies also indicated the presence of cerium in peroxisomes in controls, as well as in KCl- and sorbitol-treated cells. The most intensive EEL spectra (highest amounts) were found in electron-dense precipitates at the plasma membrane of KCl-treated cells when compared to EEL spectra acquired at other organelles (Figs. 3d, e, g, h) where precipitates were not detected.

TEM micrographs did not reveal any ultrastructural changes in organelles of treated cells compared to controls (Fig. 3a, c, f) nor did the pretreatment with cerium affect the ultrastructural appearance. As shown in a previous study (Affenzeller et al. 2009a), long-term treatment with KCl causes ultrastructural changes in mitochondria, Golgi, and ER, as well as formation of autophagosomes.

Discussion

In the present study, we investigated ROS production and putative differences in H_2O_2 localization after 15 min treatment of *Micrasterias* cells with KCl or sorbitol in comparison to controls. As published recently (Affenzeller et al. 2009a, b), KCl shows pronounced effects on viability, photosynthetic efficiency, DNA degradation, and ultrastructure of *Micrasterias* cells and, consequently, induces autophagic PCD in these cells. The present study shows a significantly higher percentage of ROS production in KCl-treated cells than in sorbitol-treated cells by labeling with H_2DCFDA in confocal laser scanning microscopy. ROS such as H_2O_2, O_2^-, and OH^- are important signaling intermediates which regulate stress response in plants (Love et al. 2008). Among them, H_2O_2 receives the most attention because of its diverse role in cell growth, development, aging, and defense responses (Slesak et al. 2007). Although the actual role of H_2O_2 in organisms is still not completely clarified, its cellular function could depend on the particular organelle where it is produced (Gechev and Hille 2005; Gechev et al. 2006). Multiple production sites of H_2O_2 in plant and animal cells have been suggested in several studies (e.g., Pellinen et al. 1999; Köhler et al. 2001). ROS, including

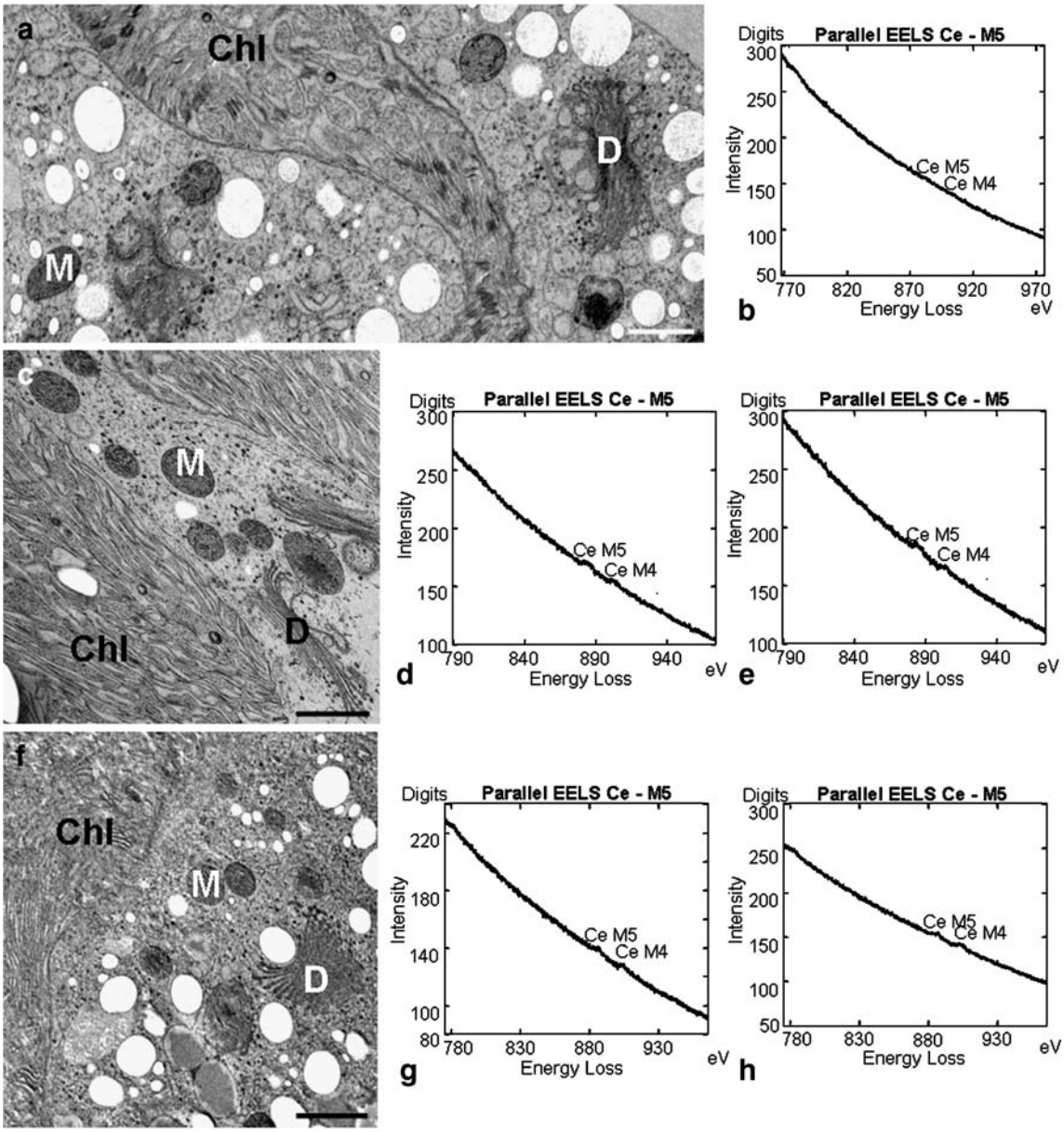

Fig. 3 TEM micrographs showing the ultrastructure of *Micrasterias* cells pretreated with $CeCl_3$ for H_2O_2 localization: **a** control cell, **c** sorbitol-treated cell, **f** KCl-treated cell. Selected examples of EEL spectra of the Ce $M_{4,5}$ edge from chloroplasts or mitochondria in treated and untreated cells: **b** chloroplast of control cell, **d** mitochondrion of sorbitol-treated cell, **e** chloroplast of sorbitol-treated cell, **g** mitochondrion of KCl-treated cell, **h** chloroplast of KCl-treated cell. *M* mitochondrion, *D* dictyosome, *Chl* chloroplast. Bar=1 μm

H_2O_2, production in plant cells after stress induction occur in chloroplasts, mitochondria, and peroxisomes by deregulation of electron transport, at the plasma membrane via activation of the plasma membrane NADPH oxidase or at the cell wall by activating cell wall peroxidases (Neill et al. 2002).

In *Micrasterias*, positive cerium measurements by EELS demonstrating H_2O_2 localization were observed in mitochondria, chloroplasts, cell walls, cytoplasm, and peroxisomes. This is particularly interesting as no precipitates were found in these regions, which means that a purely ultrastructural identification of precipitates after cerium pretreatment without EELS measurement does not provide a sufficient tool for H_2O_2 localization.

Among all organelles, the chloroplasts revealed the highest increase in H_2O_2 production after both ionic and osmotic stress in *Micrasterias*, which was statistically significant after ionic stress. ROS are generated by photosystem (PS) I and PS II in chloroplasts, which are extremely sensitive to physiological and environmental changes (Asada 2006). Our results correspond well to observations of other studies in plant cells where it has been suggested that chloroplasts have the same function in PCD as assigned to mitochondria in

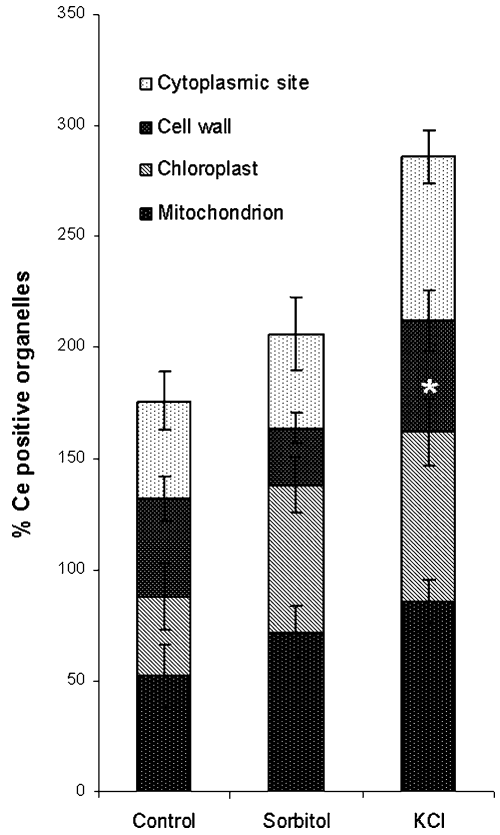

Fig. 4 Percentage of organelles in controls and sorbitol, respectively, KCl-treated *Micrasterias* cells which contain cerium in EELS analyses. Data are means of five individual cells and ten samples of each organelle in each cell +SE. *$P<0.05$

animal cells (Zapata et al. 2005; Yao and Greenberg 2006) or have even more competency than mitochondria (Martienssen 1997; Chen and Dickman 2004; Yao and Greenberg 2006). For example, in tobacco cells, it is likely that the chloroplasts are responsible for ROS production during PCD accompanying leaf senescence, whereas the mitochondria do not seem to be involved (Zapata et al. 2005).

An increase in H_2O_2 presence was also observed at cytoplasmic sites of KCl-treated cells. This could be due to an overproduction of H_2O_2 in chloroplasts and mitochondria which may consequently lead to a release of H_2O_2 from these organelles into the cytoplasm. In contrast, the H_2O_2 increase in chloroplasts and mitochondria of sorbitol-exposed cells was less pronounced. This explains the fact that no elevated levels of H_2O_2 were measured in the cytoplasm under these conditions. A decrease in H_2O_2 presence has only been observed in cell walls of sorbitol-treated cells. Plasmolysis as a consequence of sorbitol treatment could be the reason for this observation as the retraction of the plasma membrane from the cell wall may reduce the secretion of the peroxidase representing the main source of H_2O_2 in the cell wall.

In our TEM studies, H_2O_2-dependent $CeCl_3$ precipitates were observed at the plasma membranes of exclusively KCl-treated cells but never in sorbitol-treated cells or controls. EELS analyses confirmed the presence of cerium in these electron-dense precipitates. EEL spectra of these regions showed the most intensive double peaks at the cerium $M_{4,5}$ edge when compared to measurements in other organelles of KCl, respectively, sorbitol-treated cells or controls. This indicates higher amounts of H_2O_2 at the plasma membrane of KCl-treated cells than in other organelles. Several studies support the idea that the plasma membrane NADPH oxidase is involved in H_2O_2 formation after stress induction in plant cells (e.g., De Jong et al. 2002; Olmos et al. 2003; Soylu et al. 2005; Zhang et al. 2008; Wu et al. 2009). In particular, after salt stress, H_2O_2 generation by the plasma membrane NADPH oxidase has been demonstrated in wheat cells (Yang et al. 2007); this is likely to be the case in *Micrasterias* as well. According to Shabala (2009), salinity increases the cytosolic free calcium concentration which leads to an activation of NADPH oxidase resulting in a raise in ROS production (Lecourieux et al. 2002; Tracey et al. 2008).

In summary, our EELS studies reveal that chloroplasts are the major source of H_2O_2 production after salt and osmotic stress induction in *Micrasterias* cells. As expected, chloroplasts and mitochondria are generally the main production sites of H_2O_2 independent of the treatment. The ionic stress by KCl causes a stronger response in *Micrasterias* cells and leads to an excessive H_2O_2 production especially in chloroplasts and at plasma membrane sites, when compared to osmotic stress by sorbitol. Identification of cerium by EELS is required for unambiguous localization of H_2O_2, whereas a purely ultrastructural localization of precipitates does not provide reliable results.

Acknowledgment We thank Matthias Affenzeller for the helpful discussions. We gratefully acknowledge the funding from the Austrian Science Fund (FWF; grant P18869-B16 to U. L.-M.).

Conflict of interest The authors declare that they have no conflict of interest.

References

Affenzeller M, Darehshouri A, Andosch A, Lütz C, Lütz-Meindl U (2009a) Salt stress-induced cell death in the unicellular green alga *Micrasterias denticulata*. J Exp Bot 60:939–954

Affenzeller MJ, Darehshouri A, Andosch A, Lütz C, Lütz-Meindl U (2009b) PCD and autophagy in the unicellular green alga *Micrasterias denticulata*. Autophagy 5(6):854–855

Aichinger N, Lütz-Meindl U (2005) Organelle interactions and possible degradation pathways visualized in high-pressure frozen algal cells. J Microsc 219:86–94

Apel K, Hirt H (2004) Reactive oxygen species: metabolism, oxidative stress, and signal transduction. Annu Rev Plant Biol 55:373–399

Asada K (2006) Production and scavenging of reactive oxygen species in chloroplasts and their functions. Plant Physiol 141:391–396

Bestwick CS, Brown IR, Bennett MHR, Mansfield JW (1997) Localization of hydrogen peroxide accumulation during the hypersensitive reaction of lettuce cells to *Pseudomonas syringae* pv *phaseolicola*. Plant Cell 9:209–221

Blokhina OB, Chirkova TV, Fagerstedt KV (2001) Anoxic stress leads to hydrogen peroxide formation in plant cells. J Exp Bot 52:1179–1190

Boka K, Orban N, Kristof Z (2007) Dynamics and localization of H_2O_2 production in elicited plant cells. Protoplasma 230:89–97

Chen S, Dickman MB (2004) Bcl-2 family members localize to tobacco chloroplasts and inhibit programmed cell death induced by chloroplast-targeted herbicides. J Exp Bot 55:2617–2623

Chen S, Olbrich A, Langenfeld-Heyser R, Fritz E, Polle A (2009) Quantitative X-ray microanalysis of hydrogen peroxide within plant cells. Microsc Res Tech 72:49–60

Costa V, Moradas-Ferreira P (2001) Oxidative stress and signal transduction in *Saccharomyces cerevisiae*: insights into ageing, apoptosis and diseases. Mol Aspects Med 22:217–246

Darehshouri A, Affenzeller M, Lütz-Meindl U (2008) Cell death upon H_2O_2 induction in the unicellular green alga *Micrasterias*. Plant Biol (Stuttg) 10:732–745

De Jong AJ, Zakimova ET, Kapchina VM, Woltering EJ (2002) A critical role of ethylene in hydrogen peroxide release during programmed cell death in tomato suspension cells. Planta 214:537–545

De Pinto MC, Paradiso A, Leonetti P, De Gara L (2006) Hydrogen peroxide, nitric oxide and cytosolic ascorbate peroxidase at the crossroad between defence and cell death. Plant J 48:784–795

Doke N, Miura Y, Sanchez LM, Park HJ, Noritake T, Yoshioka H, Kawakita K (1996) The oxidative burst protects plants against pathogen attack: mechanism and role as an emergency signal for plant bio-defence—a review. Gene 179:45–51

Eder M, Lütz-Meindl U (2008) Pectin-like carbohydrates in the green alga *Micrasterias* characterized by cytochemical analysis and energy filtering TEM. J Microsc 231:201–214

Eder M, Lütz-Meindl U (2009) Analysis and localization of pectin-like carbohydrates in cell wall and mucilage of the green alga *Netrium digitus*. Protoplasma (in press)

Gechev TS, Hille J (2005) Hydrogen peroxide as a signal controlling plant programmed cell death. J Cell Biol 168:17–20

Gechev TS, Van Breusegem F, Stone JM, Denev I, Laloi C (2006) Reactive oxygen species as signals that modulate plant stress responses and programmed cell death. Bioessays 28:1091–1101

Houot V, Etienne P, Petitot AS, Barbier S, Blein JP, Suty L (2001) Hydrogen peroxide induces programmed cell death features in cultured tobacco BY-2 cells, in a dose-dependent manner. J Exp Bot 52:1721–1730

Köhler HBK, Huchzermeyer B, Martin M, De Bruin A, Meier B, Nolte I (2001) TNF-α dependent NF-kB activation in cultured canine keratinocytes is partly mediated by reactive oxygen species. Vet Dermatol 12:129–137

Lecourieux D, Mazars C, Pauly N, Ranjeva R, Pugin A (2002) Analysis and effects of cytosolic free calcium increases in response to elicitors in *Nicotiana plumbaginifolia* cells. Plant Cell 14:2627–2641

Love AJ, Milner JJ, Sadanandom A (2008) Timing is everything: regulatory overlap in plant cell death. Trends Plant Sci 13:589–995

Lütz-Meindl U (2007) Use of energy filtering transmission electron microscopy for image generation and element analysis in plant organisms. Micron 38:181–196

Lütz-Meindl U, Lütz C (2006) Analysis of element accumulation in cell wall attached and intracellular particles of snow algae by EELS and ESI. Micron 37:452–458

Martienssen R (1997) Cell death: fatal induction in plants. Curr Biol 7:534–537

Mazel A, Leshem Y, Tiwari BS, Levine A (2004) Induction of salt and osmotic stress tolerance by overexpression of an intracellular vesicle trafficking protein AtRab7 (AtRabG3e). Plant Physiol 134:118–128

Meindl U, Wittman-Pinegger D, Kiermayer O (1989) Cell multiplication and ultrastructure of *Micrasterias denticulata* (*Desmidiaceae*) grown under salt stress. Plant Syst Evol 164:197–208

Meindl U, Lancelle S, Hepler PK (1992) Vesicle production and fusion during lobe formation in *Micrasterias* visualized by high-pressure freeze fixation. Protoplasma 170:104–114

Melillo MT, Leonetti P, Bongiovanni M, Castagnone-Sereno P, Bleve-Zacheo T (2006) Modulation of reactive oxygen species activities and H_2O_2 accumulation during compatible and incompatible tomato-root-knot nematode interactions. New Phytol 170:501–512

Musetti R, di Toppi LS, Martini M, Ferrini F, Loschi A, Favali MA, Osler R (2005) Hydrogen peroxide localization and antioxidant status in the recovery of apricot plants from European Stone Fruit Yellows. Eur J Plant Pathol 112:53–61

Neill S, Desikan R, Hancock J (2002) Hydrogen peroxide signalling. Curr Opin Plant Biol 5:388–395

Olmos E, Martinez-Solano JR, Piqueras A, Hellin E (2003) Early steps in the oxidative burst induced by cadmium in cultured tobacco cells (BY-2 line). J Exp Bot 54:291–301

Paradiso A, Tommasi F, De Gara L, de Pinto MC (2005) Alteration in ascorbate and ascorbate peroxidase in programmed cell death and oxidative stress. BMC Plant Biol 5(Suppl 1):28

Pellinen R, Palva T, Kangasjarvi J (1999) Short communication: subcellular localization of ozone-induced hydrogen peroxide production in birch (*Betula pendula*) leaf cells. Plant J 20:349–356

Pinto E, Sigaud-Kutner TCS, Leitao MAS, Okamoto OK, Morse D, Colepicolo P (2003) Heavy metal-induced oxidative stress in algae. J Phycol 39:1008–1018

Schlösser UG (1982) List of strains. Ber Dtsch Bot Ges 95:181–206

Shabala S (2009) Salinity and programmed cell death: unravelling mechanisms for ion specific signalling. J Exp Bot 60:709–712

Shinogi T, Suzuki T, Narusaka Y, Park P (2002) Ultrastructural localization of hydrogen peroxide in host leaves treated with AK-toxin I produced by *Alternaria alternata* Japanese pear pathotype. J Gen Plant Pathol 68:38–45

Slesak I, Libik M, Karpinska B, Karpinski S, Miszalski Z (2007) The role of hydrogen peroxide in regulation of plant metabolism and cellular signalling in response to environmental stresses. Acta Biochim Pol 54:39–50

Soylu S, Brown I, Mansfield JW (2005) Cellular reactions in *Arabidopsis* following challenge by strains of *Pseudomonas syringae*: from basal resistance to compatibility. Physiol Mol Plant Pathol 66:232–243

Tipathi BN, Bhatt I, Dietz KJ (2009) Peroxiredoxins: a less studied component of hydrogen peroxide detoxification in photosynthetic organisms. Protoplasma 235:3–15

Tracey F, Gilliham M, Dodd AN, Webb AAR, Tester M (2008) NaCl-induced changes in cytosolic free Ca^{2+} in *Arabidopsis thaliana* are heterogeneous and modified by external ionic composition. Plant Cell Environ 32:1063–1073

Waetzig GH, Sobczak M, Grundler FMW (1999) Localization of hydrogen peroxide during the defence response of *Arabidopsis*

thaliana against the plant-parasitic nematode *Heterodera glycines*. Nematology 1:681–686

Wu Y, Chen Y, Yi Y, Shen Z (2009) Responses to copper by the moss *Plagiomnium cuspidatum:* hydrogen peroxide accumulation and the antioxidant defense system. Chemosphere 74:1260–1265

Yang Y, Xu S, An L, Chen N (2007) NADPH oxidase-dependent hydrogen peroxide production, induced by salinity stress, may be involved in the regulation of total calcium in roots of wheat. J Plant Physiol 164:1429–1435

Yao N, Greenberg JT (2006) *Arabidopsis* ACCELERATED CELL DEATH2 modulates programmed cell death. Plant Cell 18:397–411

Zapata JM, Guera A, Esteban-Carrasco A, Martin M, Sabater B (2005) Chloroplasts regulate leaf senescence: delayed senescence in transgenic ndhF-defective tobacco. Cell Death Differ 12:1277–1284

Zhang H, Xia Y, Wang G, Shen Z (2008) Excess copper induces accumulation of hydrogen peroxide and increases lipid peroxidation and total activity of copper-zinc superoxide dismutase in roots of *Elsholtzia haichowensis*. Planta 227:465–475